JOC*Article*

Substituent Effects in Benz[*a*]anthracene Carbocations: A Stable Ion, Electrophilic Substitution (Nitration, Bromination), and DFT Study†

Kenneth K. Laali,* Maria A. Arrica, and Takao Okazaki

Department of Chemistry, Kent State University, Kent, Ohio 44242

Ronald G. Harvey

The Ben May Institute for Cancer Research, University of Chicago, Chicago, Illinois 60637

klaali@kent.edu

Received May 4, 2007

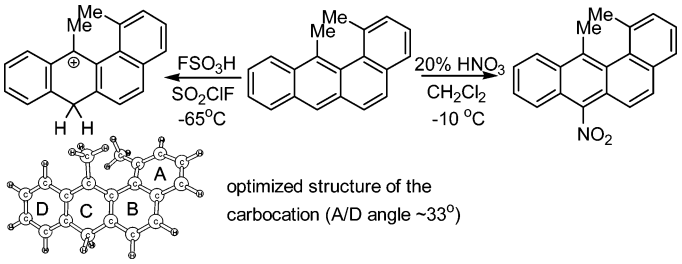

A series of novel carbocations were generated from isomeric monoalkylated and dialkylated benz[*a*]-anthracenes (BAs) by low-temperature protonation in FSO_3H/SO_2ClF. With the monoalkyl derivatives (5-methyl, 6-methyl, 7-methyl, and 7-ethyl) as well as the D-ring methylated analogues (9-methyl, 10-methyl, and 11-methyl), the C-7 or the C-12 protonated carbocations were observed (as the sole or major carbocation) in all cases. Protonation of the 12-methyl derivative (**9**) gave the C-7 protonated carbocation (**9H**$^+$) as the kinetic species and the *ipso*-protonated carbocation (**9aH**$^+$) as the thermodynamic cation. With the 12-ethyl derivative (**10**), relief of steric strain in the bay-region greatly favors *ipso*-protonation (**10aH**$^+$). With 3,9-dimethyl (**14**), C-7 protonation (**14H**$^+$) is strongly favored (with <10% protonation at C-12), and with 1,12-dimethyl (**15**) the sole species observed is the C-7 protonated carbocation (**15H**$^+$). For 7-methyl-12-ethyl, 7-ethyl-12-methyl, and 7,12-diethyl derivatives (**16**, **17**, and **18**), two *ipso*-protonated carbocations were initially formed (C-7/C-12), rearranging in time to give the C-12 protonated carbocations exclusively (**16aH**$^+$, **17aH**$^+$, and **18aH**$^+$). Protonation outcomes are compared with the computed relative energies by DFT. Charge delocalization paths in the resulting carbocations were deduced based on the magnitude of $\Delta\delta^{13}C$ values. For the thermodynamically more stable C-12 protonated carbocations, the charge delocalization path is analogous to those derived based on computed NPA charges for the benzylic carbocations formed by 1,2-epoxide (bay-region) and 5,6-epoxide (K-region) ring opening. Nitration (and bromination) of the 4-methyl, 7-methyl, 7-ethyl, 3,9-dimethyl, and 1,12-dimethyl derivatives resulted in isolation and characterization of several novel derivatives. Excellent agreement is found between low-temperature protonation selectivities and the regioselectivities observed in model substitution reactions.

Introduction

Among several classes of alternant PAHs for which structure/activity relationships have been extensively studied over the years, the benz[*a*]anthracene (BA, **1**) skeleton (Figure 1) is probably the most fascinating.[1−6]

* Address correspondence to this author. Fax: 330-672-3816. Phone: 330-672-2988.

† Dedicated to Prof. George Olah on the occasion of his 80th birthday.

(1) (a) Hecht, S. S.; Melikian, A. A.; Amin, S. In *Polycyclic Aromatic Hydrocarbons Carcinogenesis*: *Structure-Activity Relationships*; Yang, S. K., Silverman, B. D., Eds.; CRS Press: Boca Raton, FL, 1988; Vol. 1, Chapter 4. (b) Hecht, S. S.; Melikian, A. A.; Amin, S. *Acc. Chem. Res.* **1986**, *19*, 174−180.

10.1021/jo070936r CCC: $37.00
Published on Web 08/04/2007

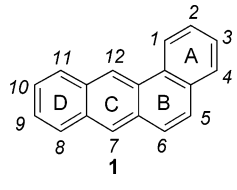

1

FIGURE 1. Benz[*a*]anthracene (BA, **1**).

Whereas parent BA is a borderline carcinogen, the 7-MBA, 12-MBA, 6-MBA, and 8-MBA derivatives are strong carcinogens, with 7-MBA being more tumorigenic than 12-MBA. Among the dimethylated derivatives, 7,12-DMBA is extremely potent. On the basis of relative carcinogenic and tumor-initiating potencies on mouse skin, the following bioactivity sequences were established for relative carcinogenicity and relative tumorigenicity respectively:[2]

7,12-DMBA > 7-MBA >
8-MBA ∼ 6-MBA ∼ 12-MBA >
9-MBA ∼ 10-MBA ∼ 11MBA >
5-MBA ∼ 1-MBA ∼ 2-MBA ∼ 3-MBA ∼ 4-MBA ∼ BA
(for relative carcinogencity)

7,12-DMBA >7-MBA > 12-MBA >
8-MBA ∼6-MBA ∼ 9-MBA > 10-MBA ∼ 11-MBA >
5-MBA ∼ 1-MBA ∼ 3-MBA > 2-MBA ∼ 4-MBA ∼ BA
(for relative tumorigenicity)

Carcinogenic activity is abolished when the Me group in 7-MBA and 12-MBA is replaced by the more bulky Et group.[4] Thus 7-EtBA and 12-EtBA did not exhibit sarcomagenic activity, and similar results were observed with the 7-OMe and 7-*n*-propyl derivatives.[4]

Focusing on the 7,12-disubstituted BA derivatives, whereas 7-Et-12-MeBA is as potent as 7,12-DMBA, 7-Me-12-EtBA had lower activity.[4,6] Carcinogenic activity of 7,12-DMBA could be completely switched off by selective fluorine introduction into the A-ring at C-1 and C-2, or by introducing a methyl group at C-2 or C-3.[5] Further methylation at C-4 or fluorine introduction into C-8 or C-11 maintained the high carcinogenic activity, but fluorination at C-4 lowered the potency.[5]

DNA binding studies on 7,12-DMBA indicated that stable adducts are formed via the bay-region diol-epoxide,[7] via 7-sulfooxymethyl, and via the 12-sulfooxymethyl derivatives.[8,9] In addition, depurinating adducts were also isolated indicating the involvement of benzylic C-12 radical cation.[10]

Using protonation as a mimic for attack by positive oxygen, in an earlier study from this laboratory,[11] we reported the first

SCHEME 1. Protonation of Methylbenz[*a*]anthracenes 2, 3, and 4 in FSO_3H/SO_2ClF

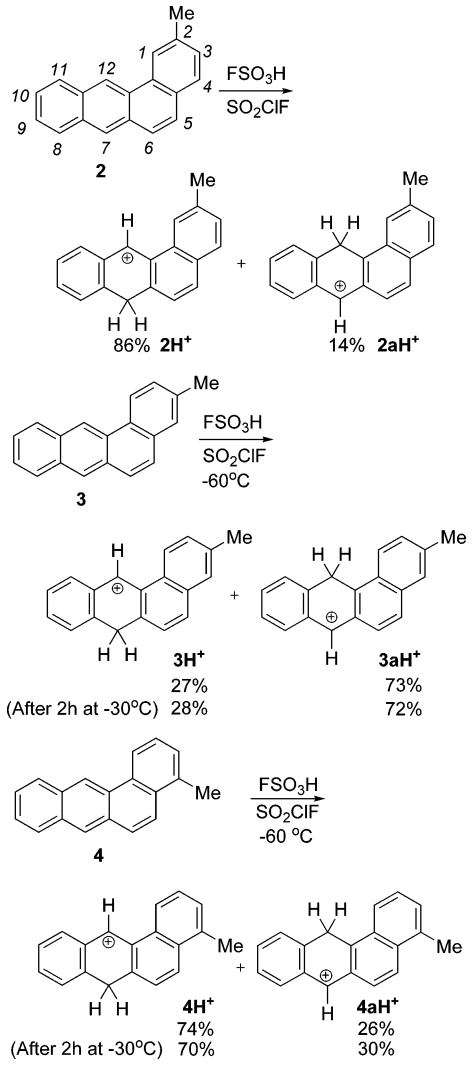

examples of stable carbocations from parent BA, 1-MBA, and 7,12-DMBA and from 3-methylcholanthrene (3-MC). Representative benzylic carbocations (α-carbocations/carboxonium ions) were also generated as models for carbocations resulting from bay-region epoxide ring opening and by benzylic epoxidation (3-MC).[11]

Since radical cation formation had been suggested as a contributing pathway in the metabolism of 7,12-DMBA, we also generated and studied by NMR the oxidation dications of 7-MBA, 12-MBA, 3-MC, 1-MBA, and BA.[12] More recently, we examined the bay-region epoxide ring process by DFT and studied substituent effects on relative carbocation stabilities, charge delocalization modes, as well as the relative energies and geometries of their guanine adducts.[13]

A more comprehensive structure/reactivity and substituent effect study has been lacking until now. Availability of a much larger set of isomeric monomethylated and dimethylated, as well as methylated-ethylated and diethylated BAs (see Figure 2), has

(2) Yang, S. K. In *Polycyclic Aromatic Hydrocarbons Carcinogenesis*: *Structure-Activity Relationships*; Yang, S. K., Silverman, B. D., Eds.; CRS Press: Boca Raton, FL, 1988; Vol. 1, Chapter 5.

(3) Harvey, R. G. *Polycyclic Aromatic Hydrocarbons*; Cambridge Monographs on Cancer Research: Cambridge, UK, 1991.

(4) Huggins, C. B.; Pataki, J.; Harvey, R. G. *Proc. Natl. Acad. Sci.* **1967**, *58*, 2253−2260.

(5) Harvey, R. G.; Dunn, F. B. *Nature* **1978**, *273*, 566−568.

(6) Pataki, J.; Balick, R. *J. Med. Chem.* **1972**, *15*, 905−909.

(7) Cheng, S. C.; Prakash, A. S.; Pigott, M. A.; Hilton, B. D.; Roman, J. M.; Lee, H.; Harvey, R. G.; Dipple, A. *Chem. Res. Toxicol.* **1988**, *1*, 216−221.

(8) Lehner, A. F.; Horn, J.; Flesher, J. W. *Polycyclic Aromat. Compd.* **2002**, *22*, 415−432.

(9) Kumar, M. N. V. R.; Vadhanam, M. V.; Horn, J.; Flesher, J. W.; Gupta, R. C. *Chem. Res. Toxicol.* **2005**, *18*, 686−691.

(10) Todorovic, R.; Ariese, F.; Devanesan, P.; Jankowiak, R.; Small, G. J.; Rogan, E.; Cavalieri, E. *Chem. Res. Toxicol.* **1997**, *10*, 941−947.

(11) Laali, K. K.; Tanaka, M. *J. Org. Chem.* **1998**, *63*, 7280−7285.

(12) Laali, K. K.; Tanaka, M. *J. Chem. Soc., Perkin Trans. 2* **1998**, 2509−2513.

(13) Borosky, G. L.; Laali, K. K. *Chem. Res. Toxicol.* **2006**, *19*, 899−907.

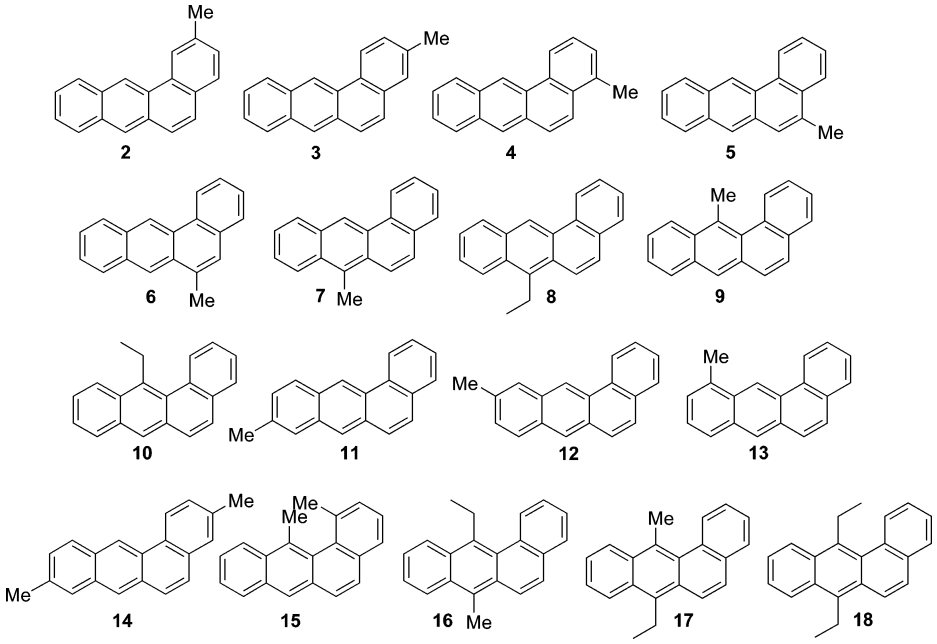

FIGURE 2. The methyl- and/or ethylbenz[*a*]anthracenes studied.

now permitted such a study, which combines stable ion NMR of the carbocations with representative electrophilic substitution study and DFT (density functional theory).

Results and Discussion

NMR Assignments of Methyl- and Ethylbenz[*a*]anthracenes. Complete ^{1}H and ^{13}C assignments for compounds **2**−**18** (Figure 2) were achieved by means of 1D and 2D NMR techniques, NOE, COSY, HMQC, and HMBC (see the Supporting Information). NMR data for 7-MBA (**7**) have been reported.[14a−c] The assignments for **7** (ref 14a) were adopted. ^{1}H NMR (in CS_2) and ^{13}C NMR (in CS_2/$CDCl_3$) data for 2-, 3-, 4-, 5-, 6-, 11-, and 12-MBA (**2**−**6**, **13**, and **9**) as well as 1,12- and 3,9-DMBA (**15** and **14**) have previously been reported.[14c] Our ^{1}H NMR data generally agreed with the reported data, except for variations in solvent effects which made some signals less deshielded in CS_2 (by 0−0.4 ppm). The previously reported ^{13}C NMR data,[14c] determined based on empirical additivity rules, are at variance with the ^{13}C NMR chemical shift reported herein.

Generation and Direct NMR Study of Carbocations from Monoalkyl-BAs. (a) A-ring alkylated substrates (Scheme 1, as well as Charts S1−S1a in the Supporting Information): Low-temperature protonation of 2-MBA (**2**) gave two carbocations by protonation at C-7 (**2H**$^+$) and C-12 (**2aH**$^+$) in 6:1 ratio, respectively. This outcome is analogous to the earlier reported protonation of 1-MBA, for which the C-7/C-12 protonated carbocation ratio was 10:1.[11] The 4-MBA (**4**) behaved analogously, generating **4H**$^+$and **4aH**$^+$ (in 2.8:1 ratio initially, slowly changing to 2.3:1). With 3-MBA (**3**) carbocations **3H**$^+$ and **3aH**$^+$ were formed, in this case favoring C-12 protonation (in 1:2.8 ratio, respectively). Based on DFT (Table S1, Supporting Information), in these systems the 7-protonated carbocations are more stable by 1.7 kcal/mol for 1-MBA, 1.8 kcal/mol for **2** (2-MBA), and 1.3 kcal/mol for **4** (4-MBA), whereas for **3** (3-MBA) the two carbocations have nearly equal energy.

Specific ^{1}H and ^{13}C NMR assignments for the resulting carbocations are given in Charts S1−S1a (Supporting Information). The H-12 (this proton exhibits NOE with H-1/H-12) in the C-7 protonated carbocations (**2H**$^+$, **3H**$^+$, and **4H**$^+$) is significantly more deshielded than H-7 (this proton exhibits NOE with H-6/H-8) in the C-12 protonated carbocations (**2aH**$^+$, **3aH**$^+$, and **4aH**$^+$). Charge delocalization paths in these carbocations (from $\Delta\delta^{13}$C values) signify a clear anthracenium ion character (within opposite/complimentary sites).

In the C-7 protonated carbocations, significant positive charge resides at C-12 (this carbon is most deshielded), whereas in the C-12 protonated carbocations the C-7 is most deshielded. The magnitude of $\Delta\delta^{13}$C (relative ^{13}C NMR chemical shifts to those of the neutrals) at C-7 in the 12-protonated carbocations is greater than that at C-12 in the 7-protonated carbocations.

(b) Substrates with a single methyl or ethyl substituent in the B- or C-ring (Scheme 2, as well as Charts S2−S2a in the Supporting Information). Protonations of 5-MBA (**5**) and 6-MBA (**6**) were directed to C-7 (**5H**$^+$ and **6H**$^+$) and protonations of 7-MBA (**7**) and 7-EtBA (**8**) were directed to C-12 (**7H**$^+$ and **8H**$^+$), selectively generating in each case only one carbocation. These outcomes are in concert with relative C-7/C-12 carbocation energies by DFT (Table S1), showing that C-7 protonated carbocations are more stable in 5-MBA and 6-MBA, whereas C-12 protonation is favored for 7-MBA. Charge delocalization modes based on $\Delta\delta^{13}$Cs in these carbocations are analogous to those in the previous group. NOE was observed in **7H**$^+$ between the methyl group and *peri*-protons (H-6/H-8) and in **8H**$^+$ between $-CH_2$-CH_3 and the *peri*-protons (H-6/H-8).

Protonation of **9** gave **9H**$^+$ and **9aH**$^+$ initially in 6.7:1 ratio in favor of C-7 protonation. However, the thermodynamically more stable *ipso*-protonated **9aH**$^+$ gradually increased in the mixture at the expense of **9H**$^+$ overtime, eventually leading to a 1:16 ratio, respectively (with **9H**$^+$ accounting for 6% of the

(14) (a) Spectral database for organic compounds by the National Institute of Advanced Industrial Science and Technology, http://www.aist.go.jp/RIODB/SDBS/. (b) Sakamoto, Y.; Aoki, T.; Ohshima, S. *Chem. Pharm. Bull.* **1996**, *44*, 424−428. (c) Jones, D. W.; Mokoena, T. T. *Spectrochim. Acta* **1982**, *38A*, 491−498.

SCHEME 2. Protonation of Alkylbenz[*a*]anthracenes 5−10 in FSO_3H/SO_2ClF

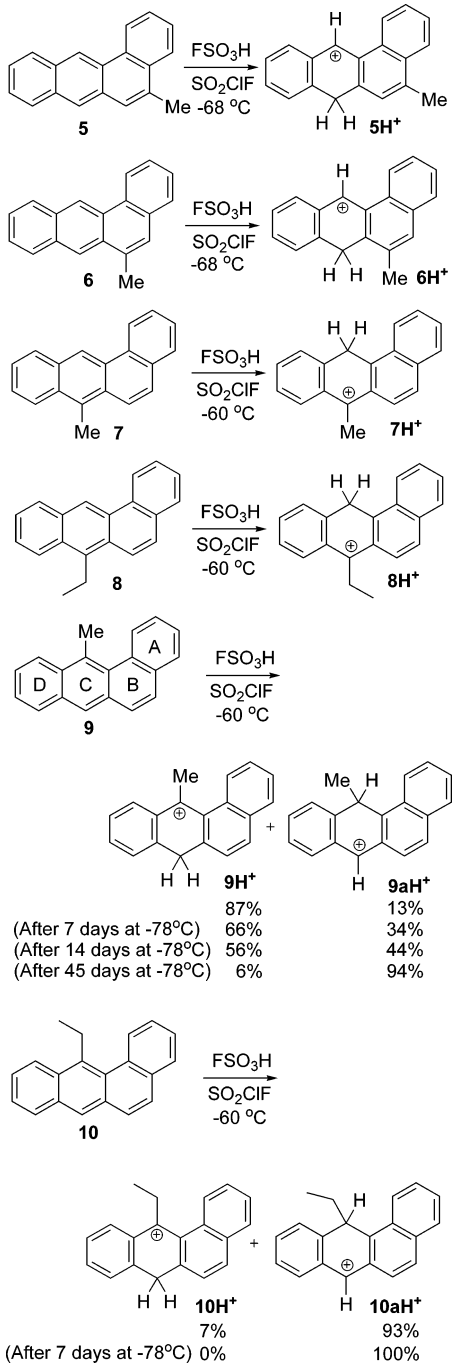

reaction mixture). DFT computed **9aH**$^+$ to be 1 kcal/mol more stable than **9H**$^+$.

Relief of bay-region steric strain in 12-EtBA (**10**) resulted in very predominant *ipso*-attack to give **10aH**$^+$ (93%). The minor **10H**$^+$ (7%) disappeared in time and **10aH**$^+$ became the sole carbocation.

Charge delocalization modes in **9H**$^+$ and **10H**$^+$ and in **9aH**$^+$ and **10aH**$^+$ are very similar. A notable feature in **9aH**$^+$ and **10aH**$^+$ is strong anisotropic shielding of the methyl protons of the ethyl group in the bay-region.

(c) Substrates with a single methyl group in the D-ring (Scheme 3, as well as Charts S3−S3a in the Supporting Information): Based on DFT, protonation at C-7 is preferred

SCHEME 3. Protonation of Methylbenz[*a*]anthracenes 11−13 in FSO_3H/SO_2ClF

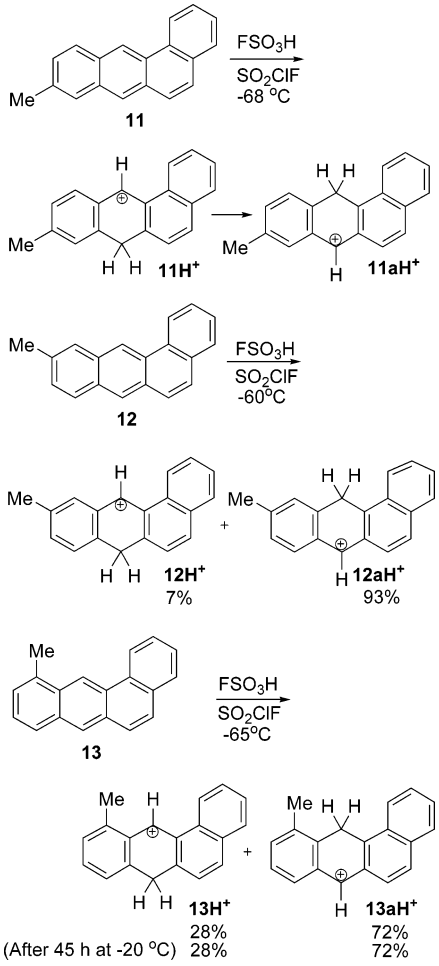

over C-12 for 9-MBA (**11**) by 3.4 kcal/mol. This did not agree with stable ion experiment, since low-temperature protonation of **11** gave **11H**$^+$ as the initially formed carbocation, which subsequently rearranged over time to **11aH**$^+$.

Protonation of 10-MBA (**12**) gave a mixture of **12H**$^+$ and **12aH**$^+$ in 1:13 ratio, strongly in favor of bay-region protonation. This outcome concurs with DFT, which places the energy of **12aH**$^+$ around 0.7 kcal/mol lower than **12H**$^+$.

Protonation of 11-MBA (**13**) gave **13H**$^+$ and **13aH**$^+$ in a 1:2.5 ratio, favoring bay-region protonation. This ratio did not change subsequently (see Scheme 3).

The methyl groups in **11H**$^+$ and **12aH**$^+$ are strategically positioned to stabilize the developing positive charge in the D-ring. Both types of carbocations exhibit clear anthracenium ion character at opposite ring positions.

Generation and Direct NMR Study of Carbocations from Dialkyl-BAs (Scheme 4, as well as Charts S4−S4a in the Supporting Information). Protonation of 3,9-DMBA (**14**) led to predominant C-7 protonation (**14H**$^+$) (with **14aH**$^+$ present in less than 10%). Only the C-9 methyl group is strategically positioned to stabilize the carbocation.

In 1,12-DMBA (**15**), the presence of two methyl groups in the bay region causes severe twisting in the skeleton. Protonation of **15** gave **15H**$^+$ as the sole carbocation. The DFT optimized structure of **15H**$^+$ is shown in Figure 3. The computed A/D twist angle is ∼33°. The ^{1}H NMR spectra for **15** and **15H**$^+$ are

SCHEME 4. Protonation of Dialkylbenz[*a*]anthracenes 14−18 in FSO_3H/SO_2ClF

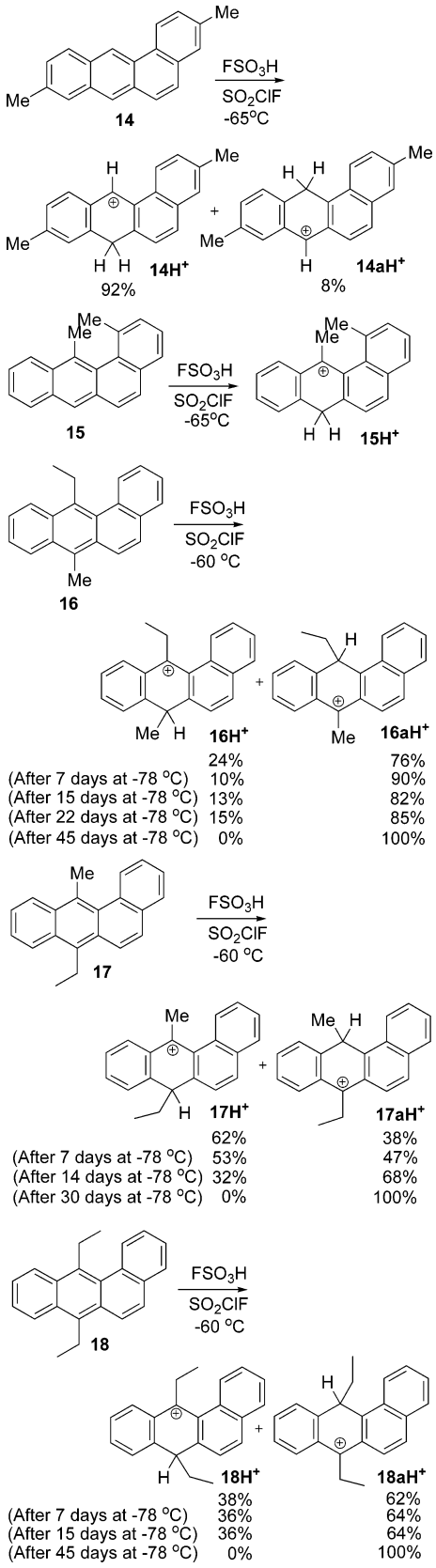

shown in Figure S1 (Supporting Information). The inset highlights the diastereotopic methylene protons as a pair of doubles.

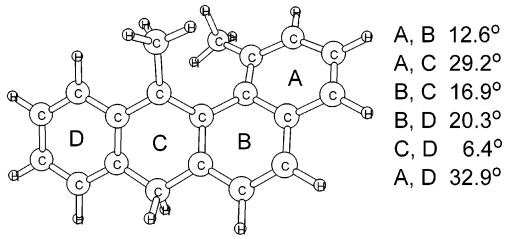

FIGURE 3. Optimized geometry and computed ring angles in **15H**$^+$ by DFT at the B3LYP/6-31G(d) level.

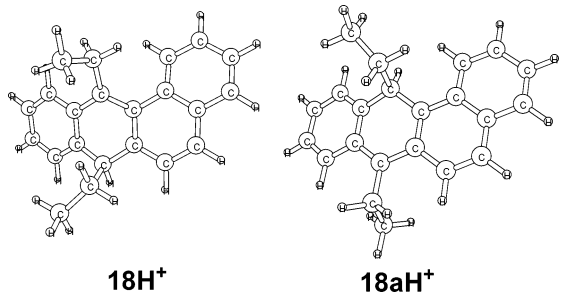

FIGURE 4. Optimized structures **18H**$^+$ and **18aH**$^+$ by B3LYP/6-31G-(d).

Interestingly, charge delocalization modes in **15H**$^+$ and **9H**$^+$ are very similar, despite increased buckling of the framework in **15**.

Protonations of the 7,12-dialkylated derivatives **16**, **17**, and **18** initially gave a mixture of the two *ipso*-protonated carbocations, favoring C-12 protonation for **16** (**16aH**$^+$) and **18** (**18aH**$^+$), and favoring C-7 protonation for **17** (**17H**$^+$). Over time, thermodynamic control took over, thereby the C-7 protonated carbocations slowly disappeared and **16aH**$^+$, **17aH**$^+$, and **18aH**$^+$ became the sole carbocations present in solution (see Scheme 4).

When *ipso*-protonation occurs at the Et group, the methylene protons exhibit strong anisotropic shielding at both C-12 and C-7, but magnitude of shielding at the bay-region ethyl group is more severe. The DFT optimized structures of **18H**$^+$ and **18aH**$^+$ reflect the highly twisted nature of the ethyl groups. The computed structures (Figure 4) correspond to geometries in which one of the methylene protons experiences the ring current effect significantly more. This is implied in the computed GIAO proton shifts in **18H**$^+$ and **18aH**$^+$, showing one highly shielded methylene proton.

Charge delocalization maps for the *ipso*-protonated 7,12-dialkyl-BAs reflect more severe localization in the C-ring, with additional charge being delocalized into two or three other conjugated carbons (see Chart S4a, Supporting Information). The *ipso*-protonated $-CH_3$ and $-CH_2CH_3$ carbons are also notably deshielded relative to their precursors ($\Delta\delta^{13}C = 14.9$ for **16H**$^+$, 16.3 for **16aH**$^+$, 15.4 for **17H**$^+$, 10.7 for **17aH**$^+$, 16.7 for **18H**$^+$, and 14.7 for **18aH**$^+$).

Model Electrophilic Substitution Reactions (Scheme 5). In agreement with the low-temperature protonation outcome, favoring electrophilic attack at C-7, mild nitration of the 4-MBA **4** gave a 5:1 mixture (91% combined isolated yield) of the isomeric mononitro products **4NO$_2$** and **4aNO$_2$**. Mild bromination of **4** led to bromination at C-7 producing **4Br** as the sole product in 89% isolated yield. Mild nitration of 7-MBA **7** and 7-EtBA **8** gave the corresponding mononitrated derivatives **7NO$_2$** and **8NO$_2$** by attack at C-12 (in 52% and 67% isolated

yields, respectively). These outcomes fully agree with the low-temperature protonation results. Mild nitrations of the dimethylated derivatives **14** and **15** were also studied as representative cases. Nitration of **14** gave a mixture of **14NO$_2$** and **14aNO$_2$** in 5.6:1 ratio, favoring attack at C-7. This outcome is consistent with the low-temperature protonation data. Both mononitro-derivatives were subsequently isolated and characterized.

Finally, mild nitration of the twisted 1,12-DMBA (**15**) gave **15NO$_2$** (nitration at C-7) and the novel derivative was isolated in 85% yield and characterized.

Comparative Discussion of the Protonation/Nitration Outcomes and Relationship to Structure/Activity Studies. The present stable ion NMR study on an extensive set of mono- and disubstituted benzo[*a*]anthracenes, along with the DFT calculations and model electrophilic substitution study, have overwhelmingly pointed to the *meso*-positions of the anthracene moiety (C-7/C-12) as the sites for electrophile attachment in the BA skeleton.

With the noncarcinogenic, A-ring methylated derivatives 1-MBA,[11] 2-MBA (**2**), 3-MBA (**3**), and 4-MBA (**4**) (Scheme 1), mixtures of C-7 and C-12 carbocations were formed, favoring C-7 protonation (except for 3-MBA). The initial carbocation ratios did not change subsequently. Model reactions (nitration and bromination) on 4-MBA gave the C-7 substituted derivatives.

The 6-, 7-, 8-, and 12-monomethyl-derivatives of BA are carcinogenic, whereas the bulkier 7-EtBA and 12-EtBA were found to be inactive.[4] The C-7 protonated carbocations were formed with 5-MBA (**5**) and 6-MBA (**6**), and the C-12 protonated carbocations were generated from 7-MBA (**7**) and 7-EtBA (**8**) as the sole species (Scheme 2). The carbocation data for 7-MBA (**7**) and 7-EtBA (**8**) concur with the nitration data (Scheme 5).

With 12-MBA (**9**) and 12-EtBA (**10**) the *ipso*-protonated carbocations are thermodynamically more stable, and the C-7 protonated carbocations which were initially present in the mixture disappeared in time. Protonation outcomes for the D-ring methylated analogues (9-MBA, 10-MBA, and 11-MBA) (Scheme 3) demonstrated strong preference for attack at C-12.

Focusing on the dialkyl-BAs (Scheme 4), protonation of 3,9-DMBA (**14**) and the highly twisted 1,12-DMBA (**15**) occurred predominantly or exclusively at C-7. The highly twisted framework of **15H$^+$** rendered the CH_2 protons diastereotopic.

Most interesting were the 7,12-dialkylated derivatives, 7-Me-12-EtBA (**16**), 7-Et-12-MeBA (**17**), and 7,12-DEBA (**18**), which extend the earlier studied 7,12-DMBA.[11] In all cases, carbocations resulting from *ipso*-attack at C-12 are thermodynamically more stable (Scheme 4). The driving force for this stability is relief of steric crowding at the bay-region. The methylene protons of the ethyl group in the *ipso*-protonated carbocations exhibited strong anisotropic shielding, reflecting a solution conformation in which the methyl protons lean over the π-framework.

The NPA-derived changes in charges for the carbocation formed via bay-region epoxide ring opening and via K-region epoxide ring opening are sketched in Figure 5.

It can be seen that the charge pattern in both cases is analogous to that derived from electrophilic attack at C-12, i.e., the thermodynamically more stable carbocations (compare NPA-derived charge patterns in Figure 5 with $\Delta\delta^{13}$C values for **16aH$^+$**, **17aH$^+$**, and **18aH$^+$** in Chart S4a, Supporting Information). Therefore, the C-12 protonated carbocations serve as good models for carbocations derived from bay-region and K-region epoxides.

SCHEME 5. Nitration and Bromination of Alkylbenz[*a*]anthracenes

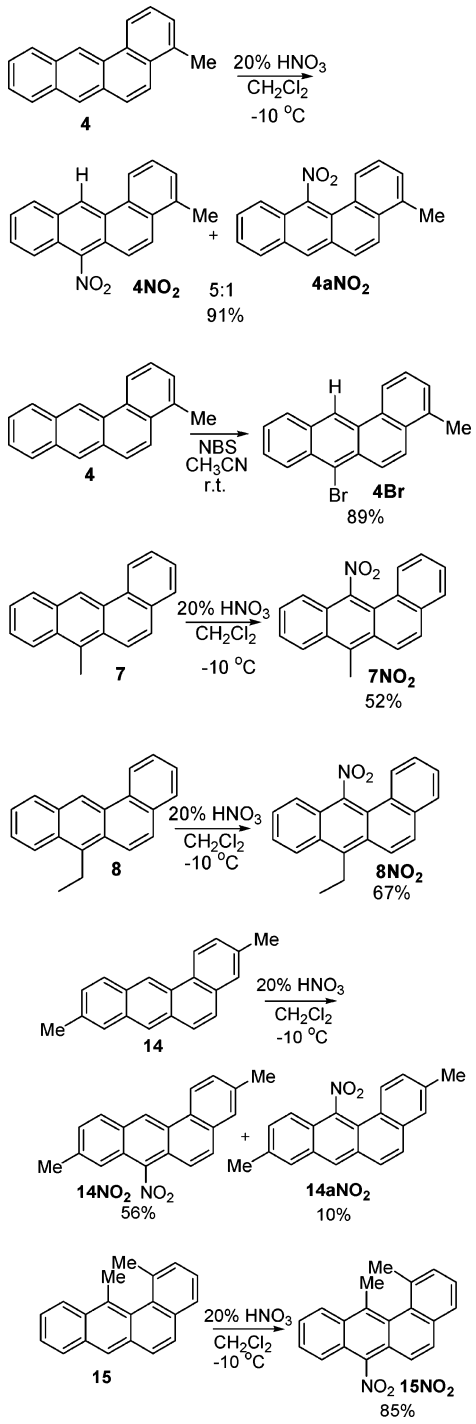

Closing Remarks on the Structure/Activity Data in the BA System. As mentioned earlier, the mechanisms invoked for 7,12-DMBA metabolism are diol-epoxide, 7-sulfooxymethyl-, and 12-sulfooxymethyl- and the radical cation formation. Diminished activity in **16** relative to 7,12-DMBA could stem from increased steric hindrance to bay-region epoxidation and blocking of the sulfooxymethyl channel and the benzylic radical cation pathway at C-12. Metabolism of **18** is likely inhibited due to steric inhibition to epoxidation at the bay-region and/or

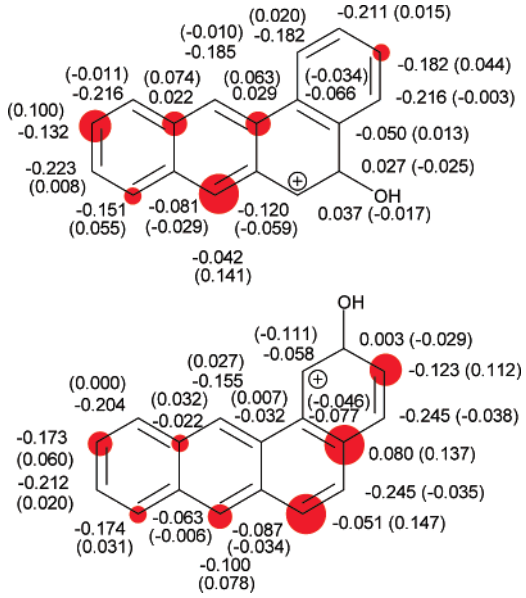

FIGURE 5. Computed NPA heavy atom charge densities for the carbocations generated from BA-1,2-epoxide and BA-5,6-epoxide by B3LYP/6-31G(d) (Δcharges relative to the corresponding epoxides in parentheses) [dark red circles are roughly proportional to the magnitude of *C* Δcharges; the threshold was set to 0.030].

K-region. For **17**, diminished activity may be a consequence of increased steric crowding at the K-region and inhibition of sulfooxymethyl channel at C-7, but bay-region epoxidation and sulfooxymethyl activation at C-12 are still possible. Lack of activity in 7-EtBA **8** is remarkable, since the bay-region epoxidation channel is potentially still open. In considering these structure/activity data in the literature, it should be realized that formation of oxidized metabolites per se does not guarantee DNA binding, since an essential part in the process is intercalation into DNA,[15] for which the thickness and the overall geometry of the PAH are believed to be decisive.[4]

Experimental Section

Carbocation Generation in FSO_3H/SO_2ClF. The substrate (10−15 mg) was placed in a 5 mm NMR tube previously flashed with argon. Into the NMR tube, cooled in a dry ice acetone bath (−78 °C), SO_2ClF (1 mL) was condensed. FSO_3H (3−4 drops) was then added under an argon atmosphere at dry ice−acetone temperature. The resulting colored solution (see below) was efficiently mixed (vortex mixer). Finally a few drops (3−4 drops) of cold CD_2Cl_2 were added to the NMR tube. The resulting solution was once again mixed (vortex) prior to NMR study. The color of the carbocation solutions varied with substituents: deep-violet for 2-MBA (**2**), 4-MBA (**4**), 5-MBA (**5**), 6-MBA (**6**), and 9-MBA (**11**); deep red for 3-MBA (**3**); brilliant red for 11-MBA (**13**) and 7-Et-12-MeBA (**17**); burgundy red for 7-MBA (**7**), 7-EtBA (**8**), 12-MBA (**9**), 12-EtBA (**10**), 10-MBA (**12**), 1,12-DMBA (**15**), 7,12-DEBA (**18**), and 7-Me-12-EtBA (**16**); and deep purple for 3,9-DMBA (**14**).

The resulting carbocations proved to be quite stable. Cold superacid solutions were stored for several weeks at dry ice−acetone temperature or at −20 °C in order to evaluate changes in carbocation ratios.

(15) See, for example: Jerina, D. M.; Sayer, J. M.; Yeh, H. J. C.; Liu, X.; Yagi, H.; Schurter, E.; Gorenstein, D. *Polycyclic Aromat. Compd.* **1996**, *10*, 145−152. Lin, C. H.; Huang, X.; Kolbanovskii, A.; Hingerty, B. E.; Amin, S.; Broyde, S.; Geacintov, N. E.; Patel, D. J. *J. Mol. Biol.* **2001**, *306*, 1059−1080. Yan, S.; Shapiro. R.; Geacintov, N. E.; Broyde, S. *J. Am. Chem. Soc*. **2001**, *123*, 7054−7066. von Szentpaly, L.; Shamovksy, I. L. *Mol. Pharmacol*. **1995**, *47*, 624−629.

General Procedure for Nitration of Methylbenz[*a*]anthracenes. Aqueous HNO_3 (20%; 1 mL) was added to a solution of methylbenz[*a*]anthracene (10 mg) in CH_2Cl_2 (1 mL) at −10 °C. The progress of the reaction was monitored by TLC until the starting material was totally consumed (usually 10−30 min). The reaction mixture was diluted with water and extracted with CH_2Cl_2 (3 × 10 mL). The combined organic extracts were then dried over $MgSO_4$. Evaporation of the solvent gave a crude product that was further purified by SiO_2 preparative thin layer chromatography (TLC).

An isomeric mixture of 4-methyl-7-nitrobenz[*a*]anthracene (**4NO$_2$**) and 4-methyl-12-nitrobenz[*a*]anthracene (**4aNO$_2$**) was co-isolated as a bright yellow solid after preparative TLC purification, using a mixture of dichloromethane−hexane (1:1) as eluent in 91% isolated yield. **4NO$_2$** (major isomer): IR (KBr) 2962, 2923, 1547, 1509, 1261, 1098, 1022, 896, 804, 744 cm^{-1}; ^1H NMR (400 MHz, $CDCl_3$) δ 2.74 (3H, s, Me), 7.51 (1H, d, J = 6.8 Hz), 7.59−7.73 (4H, m), 7.93 (1H, d, J = 8.0 Hz), 8.03 (1H, d, J = 9.6 Hz), 8.15 (1H, d, J = 8.4 Hz), 8.66 (1H, d, J = 8.4 Hz), 9.28 (1H, s, H12); ^{13}C NMR (100 MHz, $CDCl_3$) δ 19.7 (CH_3), 119.1 (CH), 121.0 (CH), 121.2 (CH), 121.3 (C), 122.6 (C), 125.0 (CH), 126.6 (CH), 127.0 (CH), 127.6 (CH), 128.5 (C), 128.6 (CH), 128.7 (CH), 129.3 (C), 129.4 (CH), 129.8 (C), 131.1 (C), 135.6 (C), 142. 3 (C); ES-MS 683.2/681.3 $[2M + Ag]^+$, 396.2/394.2 $[M + Ag]^+$; MS/MS (683/681) → 396.1/394.2 $[M + Ag]^+$ and 350.1/348.1 $[M - NO_2 + Ag]^+$.

4aNO$_2$ (minor isomer): ^1H NMR (400 MHz, $CDCl_3$) δ 8.47 (1H, s, H-7), 8.27 (1H, dd, J = 3.5 and 6.5 Hz), 8.07 (1H, d, J = 8.5 Hz), 7.91 (1H, d, J = 9.5 Hz), 7.87 (1H, d, J = 8.5 Hz), 7.79 (1H, d, J = 9.5 Hz), 7.73−7.50 (4H, m), 2.74 (3H, s); ^{13}C NMR (100 MHz, $CDCl_3$) δ 130.0 (CH), 129.3 (CH), 127.2 (CH), 126.8 (CH), 126.4 (CH), 124.2 (CH), 123.0 (CH), 121.5 (CH), 20.3 (CH_3) (two *C*Hs and quaternary *C*s not detected).

Bromination of 4-Methylbenz[*a*]anthracene (4). To a solution of 4-methylbenz[*a*]anthracene (**4**; 18 mg, 0.08 mmol) in CH_3CN (2 mL) was added *N*-bromosuccinimide (NBS, 1.3 equiv) at room temperature. The progress of the reaction was monitored by TLC. Once the starting material was totally consumed, water was added and the organic materials were extracted with CH_2Cl_2 (3 × 10 mL). The combined organic extracts were then dried over $MgSO_4$. Evaporation of the solvent gave a crude product that was purified by preparative TLC with hexane as eluent to give 7-bromo-4-methylbenz[*a*]anthracene (**4Br**)[16] as pale yellow crystals in 89% yield: IR (KBr) 3008, 2996, 1663, 1620, 1116, 802, 736 cm^{-1}; ^1H NMR (400 MHz, $CDCl_3$) δ 2.76 (3H, s, Me), 7.48 (1H, d, J = 7.2 Hz), 7.57−7.61 (2H, m), 7.66 (1H, dt, J = 8.8 and 1.2 Hz), 7.97 (1H, d, J = 9.6 Hz), 8.09 (1H, d, J = 8.4 Hz), 8.40 (1H, d, J = 9.6 Hz), 8.54 (1H, d, J = 8.4 Hz), 8.69 (1H, d, J = 8.4 Hz), 9.21 (1H, s, H12); ^{13}C NMR (100 MHz, $CDCl_3$) δ 19.7 (CH_3), 121.2 (CH), 122.2 (CH), 123.1 (C), 125.0 (CH), 125.9 (CH), 126.0 (CH), 126.9 (CH), 127.3 (CH), 127.5 (CH), 128.8 (CH), 128.9 (CH), 129.1 (C), 129.9 (C), 130.1 (C), 130.2 (C), 130.8 (C), 132.3 (C), 135.2 (C); ES-MS:750.9/748.9 $[2M + Ag]^+$; MS/MS (751/749) → 428.7/426.7 $[M + Ag]^+$, and 319.8 $[M]^+$.

7-Methyl-12-nitrobenz[*a*]anthracene (7NO$_2$). **7NO$_2$** was isolated as a bright yellow solid after preparative TLC purification, using a mixture of dichloromethane−hexane (7:3) as eluent in 52% yield: IR (KBr) 2924, 1655, 1620, 1523, 1383, 1109, 807, 755 cm^{-1}; ^1H NMR (400 MHz, $CDCl_3$) δ 3.17 (3H, s, Me), 7.59−7.74 (5H, m), 7.88−7.92 (2H, m), 8.15 (1H, d, J = 9.6 Hz), 8.37−8.44 (2H, m); ^{13}C NMR (100 MHz, $CDCl_3$) δ 29.7, 122.1, 122.8, 124.6, 125.2, 126.8, 127.7, 128.2, 128.3, 128.5, 129.0 (quaternary *C*s not

(16) Mikhailov, B. M.; Kozminskaya, T. K. *Zh. Obshch. Khim.* **1953**, *23*, 1220−1224; CA 47:72727.

detectable); ES-MS *m*/*z* 683.1/681.2 $[2M + Ag]^+$, 396.1/394.1 $[M + Ag]^+$; MS/MS (683/681) → 396.1/394.2 $[M + Ag]^+$, and 350.1/348.1 $[M - NO_2 + Ag]^+$.

7-Ethyl-12-nitrobenz[*a*]anthracene (8NO$_2$). 8NO$_2$ was obtained as a bright yellow solid after preparative TLC purification, using a mixture of dichloromethane−hexane (7:3) as eluent in 67% yield (still contained traces of unknown impurities in proton NMR; mp 133.0−135 °C): IR (KBr) 2925, 1655, 1624, 1520, 1346, 1111 cm^{-1}; ^{1}H NMR (400 MHz, $CDCl_3$) δ 1.49 (3H, t, J = 7.6 Hz, Me), 3.68 (2H, q, J = 7.6 Hz, CH_2), 7.59−7.75 (5H, m), 7.86−7.93 (2H, m), 8.12 (1H, d, J = 9.6 Hz), 8.36−8.43 (2H, m); ^{13}C NMR (100 MHz, $CDCl_3$) δ 15.4 (CH_3), 22.1 (CH_2), 122.2 (CH), 122.4 (CH), 123.6 (C), 124.2 (CH), 125.1 (CH), 126.5 (C), 126.9 (CH), 127.7 (CH), 128.2 (CH), 128.5 (CH), 129.9 (CH), 129.4 (C), 132.9 (C), 140.1 (C) (other quaternary *C*s not detectable); ES-MS *m*/*z* 711.3/ 709.2 $[2M + Ag]^+$, 410.1/408.1 $[M + Ag]^+$; MS/MS-(711) → 408.2 $[M + Ag]^+$ and 362.1 $[M - NO_2 + Ag]^+$.

3,9-Dimethyl-7-nitrobenz[*a*]anthracene (14NO$_2$). 14NO$_2$ was isolated as a bright yellow solid after preparative TLC purification, using a mixture of dichloromethane−hexane (1:1) as eluent in 56% yield: mp 193.0−196.0 °C; IR (KBr) 3010, 2919, 1627, 1514, 1368, 1112, 819 cm^{-1}; ^{1}H NMR (400 MHz, $CDCl_3$) δ 2.58 (3H, s, Me), 2.59 (3H, s, Me), 7.46 (1H, dd, J = 8.4 and 1.2 Hz), 7.56 (1H, dd, J = 8.4 and 2.0 Hz), 7.62−7.68 (3H, m), 7.74 (1H, d, J = 9.2 Hz), 8.06 (1H, d, J = 8.4 Hz), 8.67 (1H, d, J = 8.0 Hz), 9.21 (1H, s, H12); ^{13}C NMR (100 MHz, $CDCl_3$) δ 21.4 (CH_3), 22.4 (CH_3), 119.4 (CH), 119.7 (CH), 121.5 (C), 122.7 (CH), 124.0 (CH), 127.2 (C), 127.9 (C), 128.4 (CH), 128.8 (CH), 129.4 (CH), 129.6 (CH), 129.9 (C), 130.8 (CH), 131.2 (C), 137.9 (C), 138.9 (C), 143.1 (C); ES-MS 711.3/709.3 $[2M + Ag]^+$, 410.1/408.2 $[M + Ag]^+$; MS/MS (711) → 410.1 $[M + Ag]^+$, 364.1 $[M - NO_2 + Ag]^+$, and 301.2 $[M]^+$.

3,9-Dimethyl-12-nitrobenz[*a*]anthracene (14aNO$_2$). 14aNO$_2$ was isolated as a bright yellow solid after preparative TLC, using a mixture of dichloromethane−hexane (1:1) in 10% yield: IR (KBr) 3010, 2919, 1621, 1102, 970, 806 cm^{-1}; ^{1}H NMR (400 MHz, $CDCl_3$) δ 2.55 (3H, s, Me), 2.60 (3H, s, Me), 7.44 (1H, dd, J = 8.4 and 2.0 Hz), 7.53 (1H, dd, J = 9.2 and 2.0 Hz), 7.60 (1H, d, J = 9.6 Hz), 7.66 (1H, br s), 7.70−7.78 (2H, m), 7.83 (1H, br s), 8.24 (1H, d, J = 8.0 Hz), 8.37 (1H, s, H7); ^{13}C NMR (100 MHz, $CDCl_3$) δ 21.3 (CH_3), 21.7 (CH_3), 121.2 (CH), 124.5 (CH), 126.2 (CH), 126.7 (CH), 128.3 (CH), 128.5 (CH), 129.2 (2CH), 131.2 (CH) (quaternary carbons not detectable); ES-MS 711.3/709.3 $[2M + Ag]^+$, 410.1/408.2 $[M + Ag]^+$; MS/MS (711) → 410.1 $[M + Ag]^+$, 364.1 $[M - NO_2 + Ag]^+$, and 255.0 $[M - NO_2]^+$.

1,12-Dimethyl-7-nitrobenz[*a*]anthracene (15NO$_2$). 15NO$_2$ was obtained as a bright yellow solid after preparative TLC purification, using a mixture of dichloromethane−hexane (7:3) as eluent in 85% yield (traces of impurities detectable in proton NMR): IR (KBr) 3010, 2962, 1611, 1096, 1020, 800 cm^{-1}; ^{1}H NMR (400 MHz, $CDCl_3$) δ 2.50 (3H, s, Me), 2.91 (3H, s, Me), 7.42 (1H, d, J = 9.2 Hz), 7.68 (1H, br d, J = 7.6 Hz), 7.52−7.57 (2H, m), 7.65 (1H, br d, J = 7.6 Hz), 7.69−7.74 (2H, m), 7.95−7.99 (1H, m), 8.28−8.33 (1H, m); ^{13}C NMR (100 MHz, $CDCl_3$) δ 20.7 (CH_3), 22.2 (CH_3), 118.8 (CH), 122.0 (CH), 122.5 (C), 123.0 (C), 124.9 (CH), 125.1 (CH), 127.0 (CH), 127.4 (CH), 127.8 (C), 128.1 (CH), 129.6 (C), 129.9 (CH), 130.9 (CH), 131.0 (C), 133.2 (C), 135.8 (C), 137.2 (C), 142.9 (C); ES-MS 711.4/709.4 $[2M + Ag]^+$, 410.2/408.2 $[M + Ag]^+$; MS/MS (711−709) → 410.1/408.2 $[M + Ag]^+$, 364.2 $[M - NO_2 + Ag]^+$, 255.0 $[M - NO_2]^+$, and 240.0 $[M - (NO_2 + CH_3)]^+$.

Acknowledgment. Support of this study under "reactive intermediates of carcinogenesis of PAHs" by the NCI of the NIH (2R15-CA078235-02A1) is gratefully acknowledged.

Supporting Information Available: ^{1}H NMR spectra for **15**, **15H**$^+$, **17**, **17aH**$^+$, and **17H**$^+$ (Figures S1 and S2); ^{1}H and ^{13}C NMR assignments for the carbocations generated from methyl- and ethylbenz[*a*]anthracenes and their $\Delta\delta^1$H and $\Delta\delta^{13}$C relative to the neutral compounds (Charts S1−S4); spectroscopic data for the neutral compounds; energies for methylbenz[*a*]anthracenes and their protonated carbocations by B3LYP/6-31G(d) (Table S1); and general experimental section. This material is available free of charge via the Internet at http://pubs.acs.org.

JO070936R